

Lateral Diffusion and Percolation in Membranes

Bong June Sung and Arun Yethiraj

Theoretical Chemistry Institute and Department of Chemistry, University of Wisconsin, Madison, Wisconsin 53706, USA
(Received 16 February 2006; published 7 June 2006)

An algorithm based on Voronoi tessellation and percolation theory is presented to study the diffusion of model membrane components (solutes) in the plasma membrane. The membrane is modeled as a two-dimensional space with integral membrane proteins as static obstacles. The Voronoi diagram consists of vertices, which are equidistant from three matrix obstacles, joined by edges. An edge between two vertices is said to be connected if solute particles can pass directly between the two regions. The percolation threshold, p_c , determined using this passage criterion is $p_c \approx 0.53$. This is smaller than if the connectivity of edges were assigned randomly, in which case the percolation threshold $p_r = 2/3$, where p is the fraction of connected edges. Molecular dynamics simulations show that diffusion is determined by percolation of clusters of edges.

DOI: [10.1103/PhysRevLett.96.228103](https://doi.org/10.1103/PhysRevLett.96.228103)

PACS numbers: 87.15.Aa, 66.10.Cb, 87.15.Vv, 87.16.Dg

The lateral diffusion of proteins and lipid molecules in cell membranes is essential to many physiological processes. For example, the mobility of receptors is an important part of the binding of hormones because this requires the cross-linking of many receptors which are distributed on the membrane. The mobility of membrane components is also essential in diffusion-controlled reactions, such as in the electron transfer reactions involving cytochromes in the mitochondria.

The cell membrane is a very heterogeneous environment with several types of lipids and peripheral and integral membrane proteins, many of which are linked to the cytoskeleton [1]. An understanding of the biophysics underpinning the transport of lipids and proteins in complex and heterogeneous environments is therefore of considerable fundamental importance, and there are several open questions. For example, the diffusion coefficient of integral membrane proteins is almost an order of magnitude smaller in cells than in artificial bilayers, and the reason for this is not well established [2]. In some cases this can be explained in terms of interactions with the cytoskeleton, but in other cases, such as glycosyl phosphatidyl inositol (GPI) linked proteins, the interaction with the cytoskeleton cannot play a significant role. While the general phenomenology of obstructed diffusion is well established, the effect of structural details has received scant attention [2]. In this Letter we investigate the diffusion of solutes in structurally complex two-dimensional systems using molecular dynamics simulations, and analyze our results using a Voronoi tessellation method and percolation theory.

Experimental investigation of the diffusion of membrane components is an active area of research. The diffusion of tagged lipids and proteins in bilayers and cells has been measured using single particle tracking [3–5] and fluorescence recovery after photobleaching [6–8]. Experiments on different systems demonstrate a diversity in dynamic behavior. For example, in some cases, an anomalous

diffusion of proteins in the plasma membrane is observed [9]; i.e., the mean-square displacement, $W(t)$, scales with time, t , as $W(t) \sim t^\alpha$, with $0.1 < \alpha < 0.9$, while in other systems [10] diffusion is Brownian on the time-scales investigated. Some experiments suggest that the anchoring of the membrane to the cytoskeleton results in a partitioning into “corrals” with a Brownian diffusion of lipids and proteins within a corral and a hopping between neighboring corrals [4], but no signature of these is seen in other experiments [10].

Three classes of theoretical models have been used for anomalous diffusion: continuous-time random walk (CTRW) [11], obstructed diffusion, and binding. In the CTRW the solute is assumed to follow a random walk, but the probability of taking a step is a power-law function of time. The exponent characterizing this waiting time distribution is simply related to the exponent α . Obstructed diffusion has been studied using lattice models where a fraction of the lattice sites are forbidden to the solute. As the concentration of obstacles is increased, the system goes through a percolation threshold which marks the transition between free and confined diffusion [12–14]. For obstacle concentrations near the percolation threshold, diffusion is anomalous at intermediate times of significant duration because the solute explores the fractal nature of the available lattice with many dead ends. To date binding models have not received much attention.

The analysis of experiments using these models is discussed in a series of insightful papers by Saxton [2,8]. The conclusion is that these models, taken individually, are not capable of explaining the dramatic decrease in diffusion coefficient observed in experiment. In addition, the universal applicability of these models is not established. For example, in lattice models the percolation threshold depends on the coordination number of the lattice, and in continuum percolation, the percolation threshold is quite high: for randomly placed nonoverlapping discs the percolation threshold occurs at an occupation fraction of 0.82,

which is much higher than the area fraction of obstacles in a membrane.

The effect of the structure of the membrane “matrix” on the diffusion of solutes has received little attention. Part of the difficulty is that this system is an example of quenched disorder and averaging over the disorder is challenging. In this Letter we construct a simple model for diffusion in the plasma membrane. We present a Voronoi tessellation [15–17] algorithm to map the pores in continuous space to an effective lattice and analyze diffusion using percolation theory [18,19]. We argue that the diffusion of solutes is equivalent to percolation of the edges of the Voronoi diagram [20–22]. We apply these methods to a simple problem of hard discs diffusion in a sea of fixed hard discs and reproduce many of the qualitative features observed in experiment.

We model the plasma membrane as a two-dimensional system with a matrix of fixed hard discs of diameter σ_m , which is used as the unit of length, and investigate the diffusion of hard discs, of diameter σ_f , in this matrix. The simulation cell is a square of the side length, L , with periodic boundary conditions, and contains N_m randomly placed nonoverlapping stationary matrix hard discs. N_f solute particles are then inserted into the cell. If the system is percolating, the particles are inserted into a percolating region as determined from the Voronoi analysis described shortly. The solute area fraction ϕ_f ($\equiv \pi\sigma_f^2 N_f/4L^2$) is fixed at 0.1, and the matrix area fraction ϕ_m ($\equiv \pi\sigma_m^2 N_m/4L^2$) is varied from 0.1 to 0.3. In the simulations reported N_m varies from 64 to 6144, depending on ϕ_m and L . Properties are averaged over 10 different realizations of the matrix. The dynamic properties are obtained from discontinuous molecular dynamics (DMD) simulations [23,24]. This method has the advantage that it is deterministic, stable over long times, and one can “replay” a simulation. The disadvantage is that hydrodynamic interactions are ignored. As a check, we also perform dynamic Monte Carlo simulations and the results are in excellent agreement with the DMD simulations.

There are three characteristic regimes of solute dynamics. For low values of ϕ_m diffusion is normal ($\alpha = 1$) at all times, and as ϕ_m is increased the diffusion becomes anomalous for intermediate times. For sufficiently large ϕ_m (above the percolation threshold) the solute particles are confined and do not diffuse. Figure 1 depicts simulation results for the time exponent in the anomalous regime, α , as a function of ϕ_m for $\sigma_f = \sigma_m$. The figure shows that normal diffusion occurs for $\phi_m \leq 0.1$ and that the solutes are confined for $\phi_m > 0.22$, with anomalous diffusion in the intermediate regime. The percolation threshold therefore occurs for $\phi_m \approx 0.22$. Note that in the “anomalous” regime below the percolation threshold the diffusion will become normal at long times, although that regime is not accessible in our simulations.

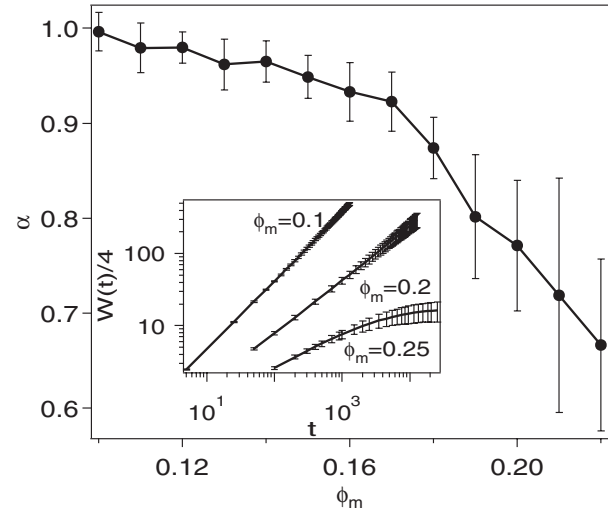


FIG. 1. Simulation results for time exponents of the mean-square displacement, $W(t)$, as a function of ϕ_m . The inset shows $W(t)$ for $\phi_m = 0.1, 0.2$, and 0.25 .

We map our model onto a lattice model using Voronoi tessellation and then analyze this using percolation theory. In Voronoi tessellation, space is divided into many non-overlapping convex polyhedra, each of which contains one matrix particle. We define the Voronoi vertices as the points that are equidistant from the three nearest matrix particles. Voronoi edges are lines that connect each vertex to the three nearest vertices. A key aspect of our construction is the manner in which we distinguish between connected and disconnected edges. Each edge has two nearest matrix particles. If the distance between these particles is less than $\sigma_m + \sigma_f$, we call this edge disconnected (because a solute particle cannot pass through), and we call the edge connected otherwise. The static correlations between matrix particles are therefore encoded in this *passage criterion* for the connectivity of the Voronoi diagram. Figure 2 depicts the Voronoi diagram for a matrix realization with $\phi_m = 0.2$. The connectivity of the edges in this case is shown for $\sigma_m = \sigma_f$. Two vertices or edges are in the same cluster if there is a connected path between them. Note that some clusters are isolated from the largest cluster, which can be percolating. A solute particle placed on this isolated cluster would be confined even if the system is percolating.

The connectivity of the Voronoi graph can be characterized by the fraction of connected edges, p , which is the number of connected edges divided by total number of edges. When either ϕ_m is increased for fixed σ_f , or σ_f is increased for fixed ϕ_m , p decreases, interestingly enough, in a roughly linear fashion. This can be seen in Fig. 3, which depicts p as a function of σ_f for $\phi_m = 0.2$ and p as a function of ϕ_m for $\sigma_f = \sigma_m$. The inset shows the exponent α for the two cases. Figure 3 shows that changing the solute size has the same qualitative effect on the

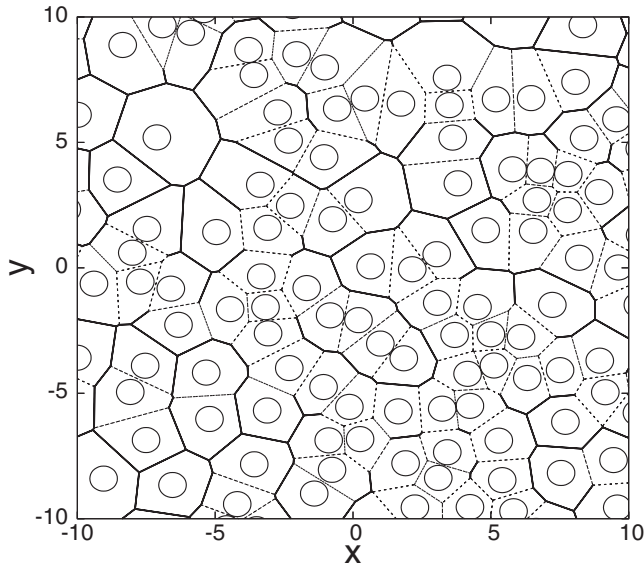


FIG. 2. Voronoi diagram for a matrix realization for $\phi_m = 0.2$. Circles represent matrix particles. Solid lines and dashed lines are connected and disconnected edges, respectively, determined using the passage criterion.

diffusion as changing the matrix area fraction. This is surprising because the structure of the solute, in terms of pair correlation functions, is quite different in the two cases. If the exponent α is plotted against p , the curves for the two models collapse onto a single curve within uncertainties (see inset).

The percolation threshold is determined by examining the mean cluster size, $S(p, L)$, defined as $S(p, L) \equiv \sum_{s=1}^{\infty} sP(s)$, where s is the number of edges in a finite cluster and $P(s)$ is the probability that an edge belongs to

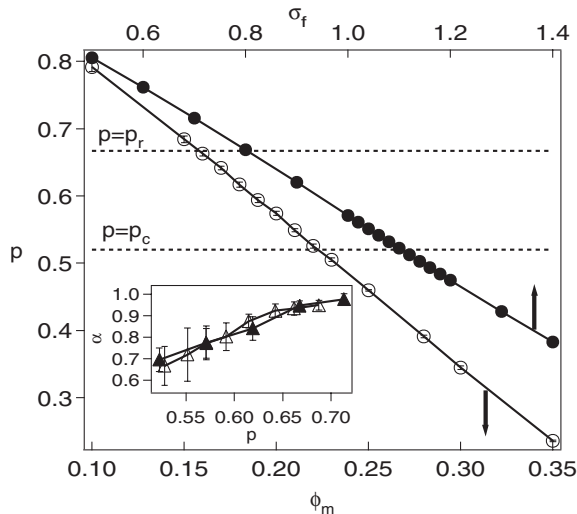


FIG. 3. Fraction of connected edges as a function of ϕ_m for $\sigma_f = \sigma_m$ (open symbols), and as a function of σ_f for $\phi_m = 0.2$ (solid symbols). The inset shows the corresponding value of the exponent α .

a cluster containing s edges [19,25]. The summation excludes percolating clusters, if any. As p is increased, $S(p, L)$ initially increases, goes through a maximum at the percolation threshold, and then decreases. As L is increased, the height of this maximum increases and diverges in the thermodynamic limit. Figure 4 depicts $S(p, L)$ for different system sizes and two cases. The solid symbols correspond to the model of this work where the connectivity is determined using the passage criterion, and with p varied by changing ϕ_m for $\sigma_f = \sigma_m$. The percolation threshold occurs for $p_c \approx 0.53$ which corresponds to $\phi_m = 0.22$. (Interestingly, an identical percolation threshold is obtained if p is varied by changing σ_f for $\phi_m = 0.2$.)

We compare the above results using the passage criterion to those of a random lattice model where the Voronoi vertices and edges are identical as above, but the connectivity of edges is assigned randomly. For each Voronoi diagram for $\phi_m = 0.2$, approximately a thousand random configurations are generated for each value of p where a fraction p of edges (chosen randomly) are assumed to be connected. The open symbols in Fig. 4 represent this model, i.e., where the edge connectivity is determined randomly. In this case, the percolation threshold, p_r , is much higher: $p_r = 0.65$, consistent with the exact result $p_r = 2/3$ [18,25]. The percolation thresholds for the passage criterion and random models, p_c and p_r , respectively, are shown as dashed lines in Fig. 3. The spatial correlations between matrix particles therefore play a very important role in determining the percolation threshold of the system.

The simulations also reconcile two pictures for the diffusion of proteins on membranes. Single molecule measurements on protein diffusion [10] show that the behavior

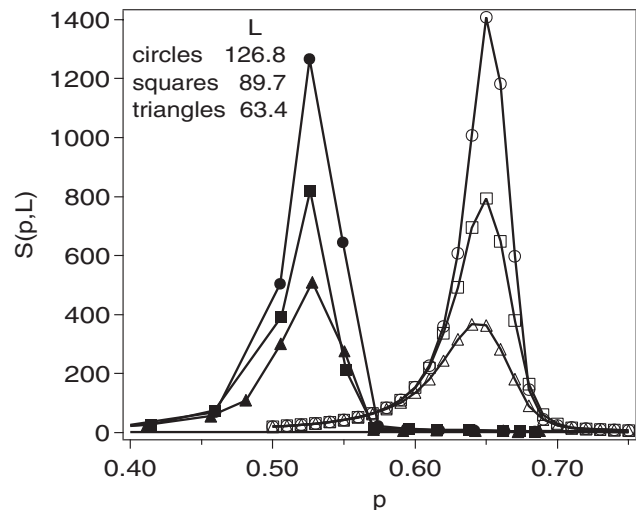


FIG. 4. Mean cluster size, $S(p, L)$, as a function of p for several system sizes. Solid and open symbols represent $S(p, L)$ for edge connectivities determined by the passage criterion (p is varied by changing ϕ_m) and for randomly connected edges, respectively.

is Brownian in all cases, while other experiments argue that the proteins are confined in *corrals* and then jump from one corral to the next [4]. The simulations show that these two pictures are not inconsistent: we observe hopping at high matrix area fractions (as has been observed for hard chains in matrices composed of hard spheres [26]) even when the long-time behavior is diffusive.

To connect with the CTRW model we calculate the waiting time distribution, i.e., the distribution of times a solute particle spends inside a Voronoi pore before moving to another pore. The heterogeneous nature of the environment results in a broad distribution of waiting times, and the distribution is nonmonotonic and decays in a roughly power-law fashion for large times. The exponent characterizing this decay is not related to the exponent α , which suggests that this model cannot be represented in terms of a CTRW.

In summary, we use Voronoi tessellation and percolation theory to study the diffusion of hard discs in a matrix of hard discs. The algorithm allows us to map the continuous-space system to a lattice and use percolation theory to study diffusion. A key aspect is that the connectivity of the bonds in the lattice is obtained from a criterion related to single particle dynamics, thus introducing local correlations into the lattice model. As the matrix area fraction is increased, the fraction of connected bonds decreases until the lattice ceases to be percolating. This percolation threshold is lower than that obtained by assigning bond connectivity randomly. The qualitative behavior is similar if the fraction of connected bonds is increased by changing the matrix density or by changing the solute size.

The extension of this approach to more complex models and phenomena is possible and promising. For example, one can estimate the lifetime of a Brownian particle hopping from one cavity to another to which it is connected by a narrow channel [27], and with this approximation the lattice model could be dressed with dynamic rules thus allowing one to estimate the diffusion coefficient without any simulations. Interactions between solute and matrix can also be incorporated into the model. Finally, one can envisage a lattice model where the matrix dynamics is taken into account. In this case, the Voronoi diagram of the matrix in terms of nodes and edges does not change, but the connectivity between nodes changes as the matrix particles move. One could mimic this by allowing some of the bonds to fluctuate between connected and disconnected as a function of time with a frequency chosen to mimic the model system. One could therefore map quite realistic systems into “barrier-crossing” lattice models.

This material is based upon work supported by the National Science Foundation under Grant No. CHE-0315219.

-
- [1] D. M. Engleman, *Nature (London)* **438**, 578 (2005).
 - [2] M. J. Saxton and K. Jacobson, *Annu. Rev. Biophys. Biomol. Struct.* **26**, 373 (1997).
 - [3] R. N. Ghosh and W. W. Webb, *Biophys. J.* **66**, 1301 (1994).
 - [4] K. Ritchie, R. Lino, T. Fujiwara, K. Murase, and A. Kusumi, *Mol. Membr. Biol.* **20**, 13 (2003).
 - [5] C. Selle, F. Ruckerl, D. S. Martin, M. B. Forstner, and J. A. Käs, *Phys. Chem. Chem. Phys.* **6**, 5535 (2004).
 - [6] T. J. Feder, I. Brust-Mascher, J. P. Slattery, B. Baird, and W. W. Webb, *Biophys. J.* **70**, 2767 (1996).
 - [7] N. Periasamy and A. S. Verkman, *Biophys. J.* **75**, 557 (1998).
 - [8] M. J. Saxton, *Biophys. J.* **81**, 2226 (2001).
 - [9] M. Wachsmuth, W. Waldeck, and J. Langowski, *J. Mol. Biol.* **298**, 677 (2000).
 - [10] M. Vrljic, S. Y. Nishimura, S. Brasselet, W. E. Moerner, and H. M. McConnell, *Biophys. J.* **83**, 2681 (2002).
 - [11] E. Montroll and G. Weiss, *J. Math. Phys. (N.Y.)* **6**, 167 (1965).
 - [12] S. Torquato and M. Avellaneda, *J. Chem. Phys.* **95**, 6477 (1991).
 - [13] S. Havlin and D. Ben-Avraham, *Adv. Phys.* **51**, 187 (2002).
 - [14] D. Ben-Avraham and S. Havlin, *Diffusion and Reactions in Fractals and Disordered Systems* (Cambridge University Press, Cambridge, 2000).
 - [15] A. Okabe, B. Boots, K. Sugihara, and S. N. Chiu, *Spatial Tessellations* (John Wiley and Sons, New York, 2000).
 - [16] M. G. Alinchenko, A. V. Anikeenko, N. N. Medvedev, V. P. Voloshin, M. Mezei, and P. Jedlovsky, *J. Phys. Chem. B* **108**, 19 056 (2004).
 - [17] V. A. Luchnikov, N. N. Medvedev, L. Oger, and J. Troadec, *Phys. Rev. E* **59**, 7205 (1999).
 - [18] S. Kirkpatrick, *Rev. Mod. Phys.* **45**, 574 (1973).
 - [19] D. Stauffer, *Phys. Rep.* **54**, 1 (1979).
 - [20] A. R. Kerstein, *J. Phys. A* **16**, 3071 (1983).
 - [21] W. T. Elam, A. R. Kerstein, and J. J. Rehr, *Phys. Rev. Lett.* **52**, 1516 (1984).
 - [22] S. C. van der Marck, *Phys. Rev. Lett.* **77**, 1785 (1996).
 - [23] M. P. Allen and D. J. Tildesley, *Computer Simulation of Liquids* (Oxford University Press, New York, 1987).
 - [24] R. Chang and A. Yethiraj, *Phys. Rev. E* **69**, 051101 (2004).
 - [25] H. Hsu and M. C. Huang, *Phys. Rev. E* **60**, 6361 (1999).
 - [26] R. Chang and A. Yethiraj, *Phys. Rev. Lett.* **96**, 107802 (2006).
 - [27] A. M. Berezhkovskii, V. Y. Zitserman, and S. Y. Shvartsman, *J. Chem. Phys.* **118**, 7146 (2003).